LRP 657/00 January 2000

Effect of triangular and elongated plasma shape on the sawtooth stability

H. Reimerdes, A. Pochelon, O. Sauter,
T.P. Goodman, M. Henderson

submitted for publication in
Plasma Physics & Controlled Fusion

ISSN 0458-5895

Effect of triangular and elongated plasma shape on the sawtooth stability

H. Reimerdes, A. Pochelon, O. Sauter, T.P. Goodman and M. Henderson

Centre de Recherches en Physique des Plasmas,
Association EURATOM - Confédération Suisse,
École Polytechnique Fédérale de Lausanne,
1015 Lausanne, Switzerland

Abstract

In the TCV tokamak the sawtooth period and the sawtooth amplitude are observed to depend strongly on the shape of the poloidal plasma cross section. Systematic scans of plasma elongation and triangularity show small sawteeth with short periods at high elongation or low and negative triangularity, and large sawteeth with long periods at low elongation or high triangularity. Additional central electron cyclotron heating power further amplifies the shape dependence of the sawtooth properties. The sawtooth period can increase or decrease with additional heating power depending on the plasma shape. This shape dependence is determined by the role of ideal or resistive MHD in triggering the sawtooth crash. For plasma shapes where additional heating and consequently a higher pressure shortens the sawtooth period, the low central pressure limit is consistent with ideal MHD predictions. The observed decrease of the central pressure limit with elongation is also in qualitative agreement with ideal MHD theory.

1 Introduction

The shaping of the poloidal plasma cross section can be used to improve tokamak performance and efficiency. In order to determine the optimum shape for a tokamak reactor the effects of shaping on confinement and on stability limits have to be considered. The sawtooth instability, characterized by an internal disruption resonant on the q=1 flux surface [1], is present in most standard tokamak scenarios and has an important effect on core confinement.

In this paper, we show the strong dependence of the sawtooth amplitude and period on plasma elongation κ and triangularity δ observed in recent TCV (Tokamak à Configuration Variable) experiments, supplementing the previous results in ohmic plasmas [2]. Furthermore, we analyze the response of sawteeth to centrally deposited electron cyclotron resonance heating (ECRH) power (preliminary results in [3]). Since the sawtooth period is determined by the evolution of the current and pressure profiles from a relaxed to a sawtooth-unstable state, it depends on transport processes, in particular the energy and the current transport, and on a stability criterion for the sawtooth crash. Both, the transport and stability criteria depend on the plasma shape, which can consequently induce variations of the sawtooth period. Sawtooth amplitude and period are linked via the core power balance. As the sawtooth period in the analyzed discharges is smaller than or equal to the energy confinement time, the re-heat of the plasma core is mainly determined by the central heating power leading to a linear sawtooth ramp.

We show that the dependence of the sawtooth period on elongation, triangularity, and heating power can be linked to the stability of the ideal MHD and resistive internal kink modes, which are deemed responsible for the internal disruption. The ideal internal kink is stabilized by toroidicity up to a critical pressure gradient [4], which can be expressed in terms of a poloidal beta on the q=1 surface defined by

$$\beta_{\mathrm{p},1} = \frac{\langle p \rangle_1 - p(r_1)}{B_{\mathrm{p}}^2(r_1)/2\mu_0} \,, \tag{1}$$

where $\langle\rangle_1$ denotes a volume average within the q=1 surface. Note that $\beta_{\mathrm{p},1} = 0$ corresponds to a flat pressure profile within q=1. The predicted stability limit of $\beta_{\mathrm{p},1} < 0.3$ for a large q=1 radius, r_1, and a circular cross section [4] is considerably lowered by elongation, with combined toroidicity and ellipticity effects being particularly important [5]. When the ideal MHD potential energy is close to zero, i.e. the equilibrium is in a state close to marginal stability, non-ideal effects like resistivity are assumed to determine the mode dynamics [6].

2 Experiment

The TCV tokamak (major radius $R = 0.88\,\mathrm{m}$, minor radius $a = 0.25\,\mathrm{m}$, vacuum vessel elongation $\kappa_{\mathrm{TCV}} = 3$) is equipped with 16 independently controlled poloidal field coils which allow for a large variety of plasma shapes. In the experiments presented in this paper the elongation was varied from 1.1 to 2.1 and the triangularity from -0.25 to $+0.45$. The flux contours of a typical discharge together with the ECRH beam location and the vacuum vessel are shown in Fig. 1(a). The sawtooth period τ_{saw} and its amplitude A_{saw} are obtained from a soft X-ray emission measurement I_{x} along a chord passing through the plasma center. The crash amplitude is normalized to the total chord intensity ($A_{\mathrm{saw}} = \Delta I_{\mathrm{x}}/I_{\mathrm{x}}$). Both characteristic sawtooth parameters are averaged over stationary intervals of typically 100 ms corresponding to 20 to 200 sawtooth periods (Fig. 1(b)). The crash amplitude can be corrected for the temperature dependence of the X-ray emissivity of the dominant impurity, carbon, using the factor $\alpha = d(\ln I_{\mathrm{X}})/d(\ln T_{\mathrm{e0}})$. This correction factor decreases from 1 at 900 eV, typical for T_{e0} in ohmic plasmas of the presented experiments, down to 0.6 at 2.5 keV in plasmas with additional heating. With density variations assumed negligible, $\alpha^{-1}A_{\mathrm{saw}}$ then provides an estimate for the relative core pressure loss due to the sawtooth crash.

In order to separate the shape dependence, other plasma parameters like the temperature, density, and current profiles, which can influence the sawtooth behaviour, have been kept similar. It has been shown that over a wide range of plasma shapes the profile broadness is related to the position of the q=1 surface or the sawtooth inversion radius ρ_{inv} [7] accordingly:

$$\langle p_{\mathrm{e}} \rangle / p_{\mathrm{e0}} \approx \rho_{\mathrm{inv}} \approx \langle j \rangle / (q_0 j_0) \ , \qquad (2)$$

where $\langle\rangle$ denotes volume averages and ρ is a normalized plasma radius defined by $\rho = (V(\rho)/V_{\mathrm{total}})^{1/2}$. The inversion radius, and consequently the profile broadness, was kept constant throughout the scanned parameter range. Experimentally this was achieved by carefully adjusting the plasma current, while the edge safety factor q_a increased with elongation from 2.5 to 3.5 and with triangularity from 2.5 to 3.0. The sawtooth inversion contour was determined from the tomographic inversion of soft X-ray emission measurements [8] and then mapped onto a flux coordinate using the reconstructed flux from the equilibrium code LIUQE [9]. For all explored shapes the inversion radius was found to be $\rho_{\mathrm{inv}} = 0.45 \pm 0.05$. The remaining variations are neither correlated with variations in shape nor heating power and are of the order of the uncertainties of the tomographic inversion and of the equilibrium reconstruction.

The electron temperature and density profile measurements were obtained from a

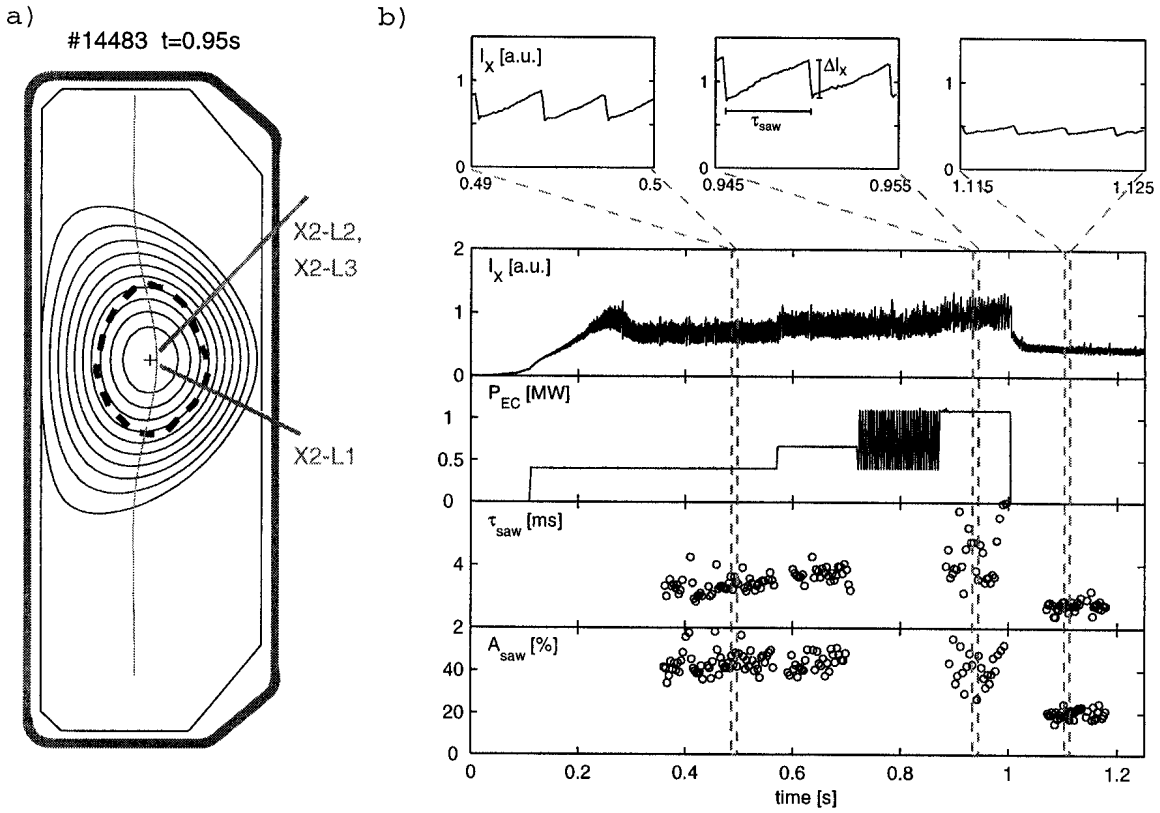

Figure 1: (a): Poloidal cross section of a plasma ($I_p = 400\,\mathrm{kA}$, $\kappa = 1.45$, $\delta = 0.45$) and ECRH launching geometry for central power deposition. The absorption layer for the X2-mode and the sawtooth inversion radius are indicated. (b): Soft X-ray emission measurements I_x along a central chord show the variations of sawteeth during the stepping up of the ECRH power. Their period τ_{saw} and crash amplitude A_{saw} are determined in intervals with constant plasma parameters.

multi-chord Thomson scattering diagnostic [10]. There are 10 to 25 measurement locations inside the plasma, depending on the plasma elongation, which are mapped onto flux coordinates. The measurements were not synchronized with the sawteeth and, therefore, the profiles have to be averaged over the stationary intervals. Since the Thomson scattering diagnostic measures with a sampling rate of 60 Hz, typically 6 profiles were used for averaging. Throughout the scanned plasma shapes, the broadness of the ohmic electron temperature profile $\langle T_e \rangle / T_{e0} = 0.57 \pm 0.05$ and electron density profile $\langle n_e \rangle / n_{e0} = 0.74 \pm 0.03$ remained constant. The values obtained for the inversion radius and profile broadness are consistent with previous work [7].

The sawtooth period also depends on particle density. For example in a moderately shaped ($\kappa \sim 1.5$, $\delta \sim 0.2$) ohmic TCV plasma τ_{saw} increased from 1.7 ms at a central electron density $n_{e0} = 1 \times 10^{19}\mathrm{m}^{-3}$ to 3.0 ms at $n_{e0} = 5 \times 10^{19}\mathrm{m}^{-3}$. However, this dependence is weak for low densities. In the narrow range of n_{e0} between 2.2 and $3.1 \times 10^{19}\mathrm{m}^{-3}$ the

period of ohmic sawteeth varied only from 1.9 to 2.2 ms. In order to exclude the influence of density, all plasmas of the shape scans have been in this narrow density range.

Auxiliary heating power was applied to increase the plasma pressure. Three 82.7 GHz, 500 kW gyrotrons for heating at the second harmonic of the electron cyclotron resonance were used in this study [11]. The chosen density range is well below the cut-off density, $n_{\text{e,cut-off}} = 4.25 \times 10^{19}\text{m}^{-3}$, of the second harmonic extraordinary mode (X2-mode). The ECRH power, P_{EC}, was increased in three steps and included an interval where the power was modulated (Fig. 1(b)). A central power deposition was chosen so as to guarantee similar effects on current and pressure profiles and increase the global pressure rather than induce local changes in the vicinity of the q=1 surface. In particular non-standard sawtooth behaviour such as *saturated, inverse*, or *humpback* sawteeth [12], which usually result from localized off-axis heating [13], were avoided. Figure 1(a) shows the X2-mode launching geometry and the resonance position for a vacuum field of 1.43 T which is increased by the paramagnetism of the plasma. Some ordinary mode (O-mode) component of the injected ECRH beam, which is weakly absorbed at first path, leads to more distributed absorption after multiple reflection on the wall. The deposition profile is obtained from the response of the soft X-ray emissivity to the switch-off of the ECRH power. The resulting deposition agrees well with the calculations from the ray-tracing code TORAY [14]. Both methods confirm a peaked power absorption in a region well inside the q=1 surface.

3 Variations of sawtooth characteristics

In a moderately shaped ($\kappa = 1.5$, $\delta = 0.2$) ohmically heated TCV plasma with $n_{e0} \approx 2.5 \times 10^{19}\text{m}^{-3}$ sawteeth typically have periods of 2 ms and crash amplitudes of 10%. Triangularity and elongation scans were performed around this shape, keeping either $\kappa \approx 1.5$ or $\delta \approx 0.2$ constant.

In ohmic plasmas the modification of the triangularity introduces significant changes of sawtooth characteristics (Fig. 2(a,c)). Increasing δ from 0 to 0.45 almost doubles the sawtooth period and increases the amplitude of the crash by a factor of 4. The modification of τ_{saw} and A_{saw} saturates for negative triangularities. As already noted in [2] the increase in amplitude with triangularity can be explained by a combined effect of a longer sawtooth period and a higher ohmic heating power density. The dependence of elongation on the sawtooth period is weaker (Fig. 2(b)), with a trend for shorter sawtooth periods at higher elongation. Despite the weak trend in the behaviour of τ_{saw} the crash amplitude decreases drastically with elongation (Fig. 2(d)). For $\kappa = 2$ the crash

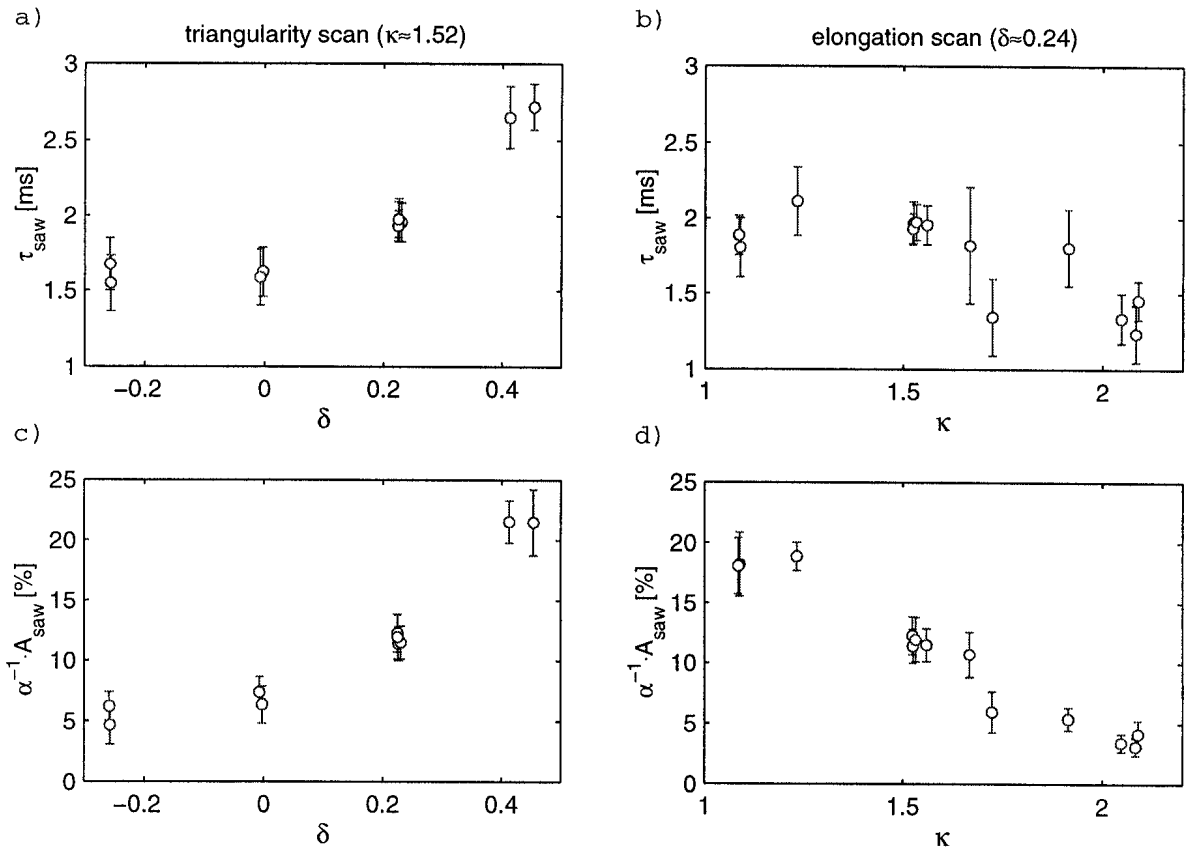

Figure 2: Sawtooth characteristics in ohmic plasmas as a function of triangularity (a,c) and elongation (b,d), while density and inversion radius are kept constant. The values of the sawtooth period (a,b) and the sawtooth crash amplitude (c,d) are averaged over stationary phases. The error bars indicate the standard deviation within these phases.

amplitude measures only a fourth of the amplitude in an almost circular plasma although the inversion radius was kept constant throughout these experiments. Again, the variation of τ_{saw} is not sufficient to explain the variation of $\alpha^{-1}A_{\mathrm{saw}}$. As for decreasing δ, the ohmic heating power density decreases with increasing κ (while ρ_{inv} is kept constant), which results in the observed drop in crash amplitude.

Central ECRH deposition enhances the effect of shape previously observed in ohmic plasmas. For high positive triangularity auxiliary heating increases τ_{saw} even further up to 4 ms and $\alpha^{-1}A_{\mathrm{saw}}$ up to 65%, where it saturates. Small and negative δ results in even shorter and smaller sawteeth (Fig. 3(a,c)). We further note that the assumption of constant density throughout the sawtooth cycle is no longer valid in ECRH heated plasmas [15] and therefore $\alpha^{-1}A_{\mathrm{saw}}$ fails as an estimate for the central pressure loss. With additional heating a distinct dependence of the sawtooth period on elongation also becomes apparent (Fig. 3(b,d)). For nearly circular plasmas the additional heating further increases τ_{saw} and A_{saw}, while at high elongation τ_{saw} and A_{saw} are decreased further below

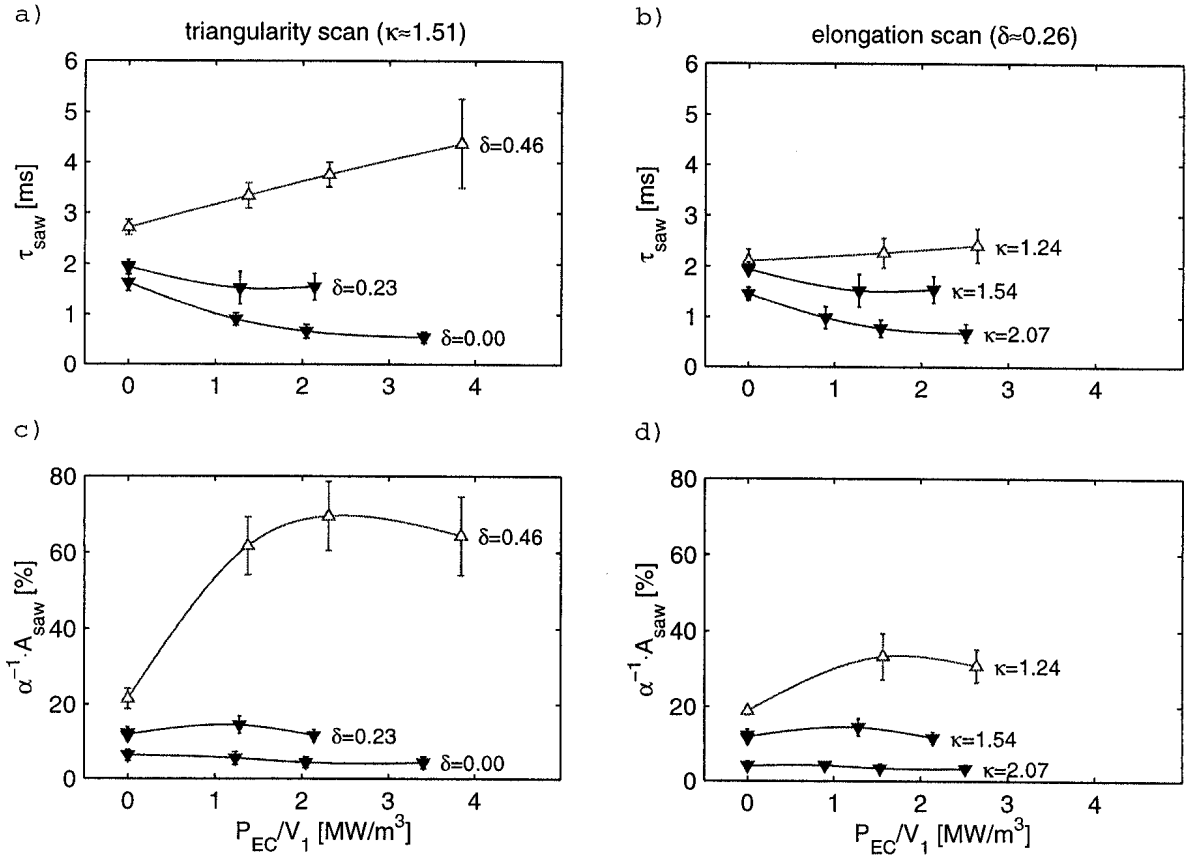

Figure 3: Sawtooth characteristics as a function of auxiliary heating power density within the q=1 surface for various triangularities (a,c) and elongations (b,d). Electron density and sawtooth inversion radius were kept constant. Shown is the dependence of sawtooth period (a,b) and the relative sawtooth crash amplitude (c,d) on ECRH power. The values are averaged over a stationary phase with the bars indicating the standard deviation within these phases.

ohmic values.

Thus, the enhancement of the effect of shape on sawtooth behaviour is due to the shape dependent response to ECRH. The shaping parameters for which the increase of P_{EC} results in a decrease of τ_{saw}, i.e. auxiliary heating is destabilizing, and the shaping parameters for which an increase of P_{EC} is stabilizing are shown in Fig. 4, clearly indicating this shape dependence.

4 Comparison with a sawtooth model

The observed response of sawteeth to heating is compared to a model, which was developed to predict the sawtooth period in JET and ITER [6] and has already successfully been applied to ohmic TCV plasmas [17].

According to this model an ideal internal kink triggers the sawtooth crash if its growth

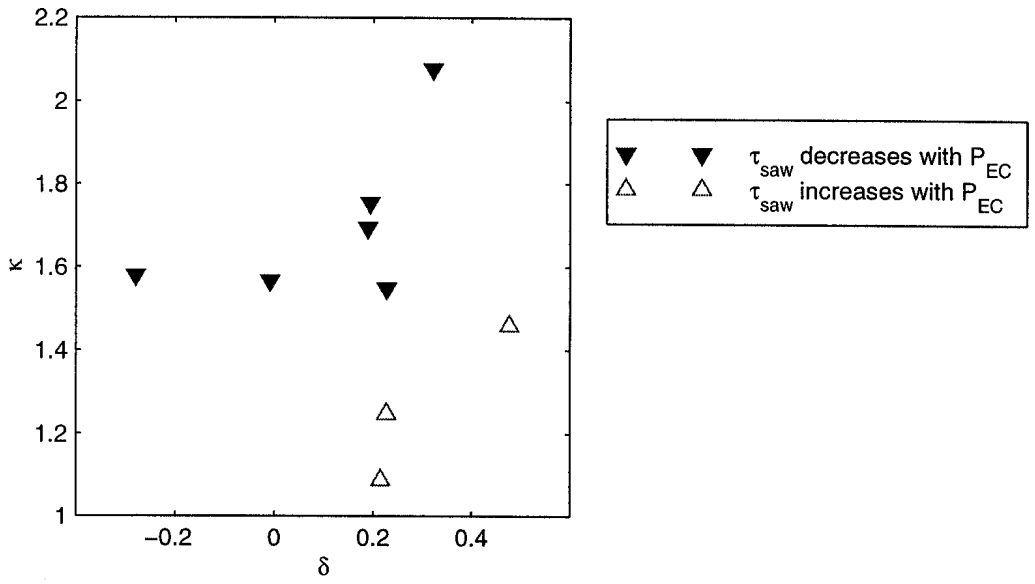

Figure 4: The discharges where τ_{saw} decreases (filled triangles) or increases (open triangles) with P_{EC} are shown as a function of shaping parameters at the plasma edge.

cannot be stabilized by plasma rotation, i.e. if

$$\gamma_{\mathrm{ideal}} = \frac{-\delta\hat{W}}{\tau_{\mathrm{A}}} > c_h w_{\mathrm{i,dia}} \tag{3}$$

where $\delta\hat{W}$ is the total potential energy of the internal kink mode, $\omega_{\mathrm{i,dia}} = kT_{\mathrm{i}}/(L_p e B_0 r_1)$ the ion diamagnetic drift frequency, τ_{A} the Alfvén time and $c_h \approx 0.5$. In a low density TCV plasma, the amplitude of the term which can stabilize the internal kink mode is typically $c_h w_{\mathrm{i,dia}} \approx 5 \times 10^3\,\mathrm{s}^{-1}$, a value which is observed to decrease with the auxiliary electron heating power. The potential energy $\delta\hat{W}$ is determined by summing the ideal MHD potential energy and by the stabilizing contribution of thermal trapped ions and fast particles

$$\delta\hat{W} = \delta\hat{W}_{\mathrm{MHD}} + \delta\hat{W}_{\mathrm{trapped}} + \delta\hat{W}_{\mathrm{fast}}. \tag{4}$$

In the presented experiments, the stabilizing effect of fast particles on sawteeth can be neglected. Also the stabilizing effect of collisionless thermal trapped ions in the present low density plasmas is small, with $\delta\hat{W}_{\mathrm{trapped}}/\tau_{\mathrm{A}}$ of the order of $5 \times 10^2\,\mathrm{s}^{-1}$. Therefore the internal kink can be destabilized by $\delta\hat{W}_{\mathrm{MHD}}$ becoming negative once the plasma pressure sufficiently exceeds a critical value. This critical value is believed to depend strongly on plasma shape [5, 16]. Thus, the additional heating increases the plasma pressure which should increase the drive of the ideal mode and result in a decrease in the sawtooth period.

If the plasma is stable with respect to the ideal mode (Eq. (3)), resistivity becomes important. In ECRH heated TCV plasmas the ion-gyro radius $\rho_i \approx 0.2 - 0.3\,\mathrm{cm}$ is larger

than the resistive layer width $\delta_\eta \approx 0.03 - 0.12\,\mathrm{cm}$ and the growth rate γ_ρ of the resistive internal kink in the so-called *ion-kinetic* regime has to be considered [12]. A typical value is $\gamma_\rho \approx 10^4 s^{-1}$. The mode can be stabilized by different diamagnetic effects leading to a condition for the onset of the resistive internal kink mode proposed in [17]:

$$c_\star \gamma_\rho > (\omega_{e,dia}\omega_{i,dia})^{1/2} \tag{5}$$

with $c_\star$ being of order unity. Since $\omega_{\mathrm{e,dia}} \approx 10^4 s^{-1}$ both sides of Eq. (5) are of similar amplitude. The resistive growth rate $\gamma_\rho \propto s_1^{6/7}$ essentially depends on the magnetic shear on the q=1 surface $s_1 = \rho_1 \, (dq/d\rho_1)$, whereas the stabilizing electron diamagnetic rotation increases with pressure. Additional ECRH increases p_e but also influences the evolution of s, leading to different dynamics with respect to the ideal mode (Eq. (3)). In particular the stabilization of a resistive mode by electron diamagnetic rotation offers a possible explanation for an increase of the sawtooth period with additional electron heating.

Therefore, the response of sawteeth to auxiliary heating is expected to depend whether ideal or resistive MHD determines the mode dynamics. As discussed above this essentially depends on the potential energy of the ideal mode $\delta\hat{W}_{\mathrm{MHD}}$, which contains the shape dependence. A necessary condition for ideal MHD stability is the Mercier criterion. Numerical simulations have shown that in elongated plasmas with weak central shear the $\beta_{p,1}$ limit is set by a violation of the Mercier criterion leading to an $n = 1$ mode with large growth rates and more importantly, that the shape dependence of $\delta\hat{W}_{\mathrm{MHD}}$ is similar to the shape dependence of the Mercier criterion [16]. In cases where the Mercier criterion was violated within the whole $q < 1$ region, the eigenfunction of the unstable mode resembles the standard step function of the internal kink. An expansion of the Mercier criterion up to second order in toroidicity $\epsilon = r/R_0$ and first order in ellipticity $e = (\kappa - 1)/2$ including the contributions of order $\epsilon^2 e$ [16] illustrates the effect of elongation and triangularity. For q=1, stability requires

$$-D_I = \frac{1}{4} - \frac{3\epsilon_1^2}{s_1^2}\left(\kappa_1 - 1\right)\beta_{p,1}\left(1 - \frac{2\delta_1}{\epsilon_1}\right) > 0. \tag{6}$$

In Fig. 5, marginal stability according to the Mercier criterion (Eq. (6)) is shown for two values of $\beta_{\mathrm{p,1}}$, with $s_1 = 0.1$ and $\rho_1 = 0.5$ assumed constant, as a function of the local shaping. The discharges in Fig. 4 are shown in Fig. 5 as a function of the local shaping parameters at q=1, which are obtained from the equilibrium reconstruction. A comparison of the sawtooth response to ECRH with the Mercier stability boundary shows that the critical $\beta_{\mathrm{p,1}}$ is particularly low for discharges where additional heating could not improve sawtooth stability (filled triangles in Fig. 5). For these plasma shapes the potential energy

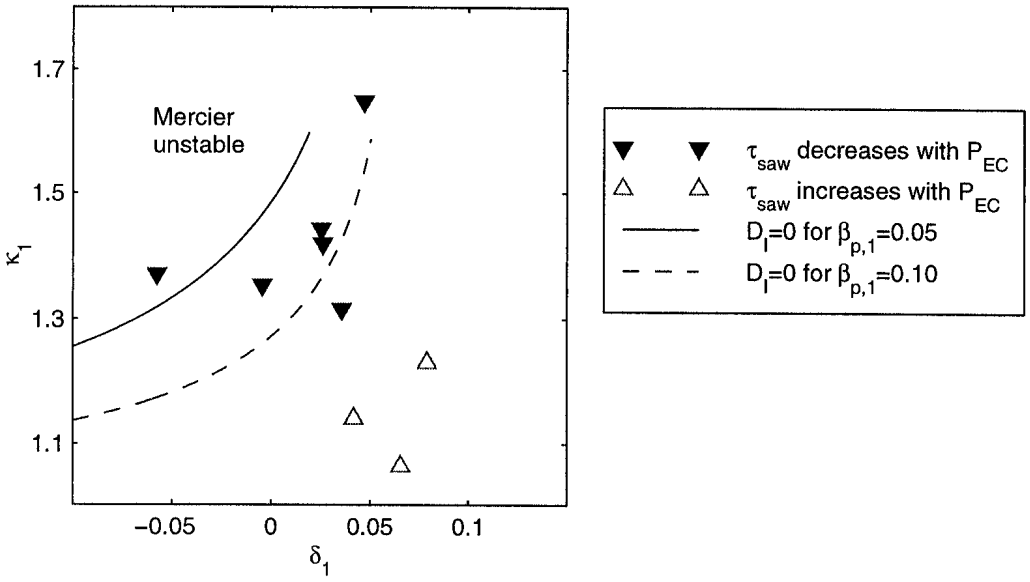

Figure 5: The discharges of Fig. 4 are shown as a function of shaping parameters on the q=1 surface. The plasma shapes are compared to the shapes corresponding to marginal stability according to the Mercier criterion (Eq. (6)) for two different values of $\beta_{p,1}$ and assuming constant shear $s_1 = 0.1$ and inversion radius $\rho_{\rm inv} = 0.5$.

of the ideal mode can be sufficiently negative to determine the sawtooth trigger which is consistent with the interpretation of the decrease of the sawtooth period presented above.

The shape dependent response of sawteeth to heating power can also be seen in the electron pressure profiles. In Fig. 6, the time averaged pressure profiles of a plasma where $\tau_{\rm saw}$ increased with $P_{\rm EC}$ (a) are compared with the profiles of a plasma where $\tau_{\rm saw}$ decreased with $P_{\rm EC}$ (b). In the first case (a) the increase of the central heating from ohmic to 1 MW of auxiliary heating power leads to a peaking of the pressure profile whereas in case (b) the central pressure profile remains essentially flat. The variation of the pressure profiles with heating can be summarized in the variation of $\beta_{\rm p,1}$, which increases with $P_{\rm EC}$ in case (a) but remains constant in case (b) (see inserts in Fig. 6). Thus, case (b) is consistent with an imposed central beta limit, independent of heating power, leading to the observed decrease of $\tau_{\rm saw}$ for this plasma shape. This supports the idea of ideal MHD being responsible for the triggering of the sawtooth. However, note that the measured betas are time averages of measurements, which were not synchronized with sawteeth and are therefore lower than the critical beta obtained right before the crash.

For all plasma shapes, where $\tau_{\rm saw}$ decreased with P_{EC}, the limiting $\beta_{\rm p,1}$ was independent of heating power (like Fig. 6(b)), whereas for the other plasma shapes $\beta_{\rm p,1}$ increased with power (like Fig. 6(a)). For the shapes where $\beta_{\rm p,1}$ reaches a limit, this limit is shown

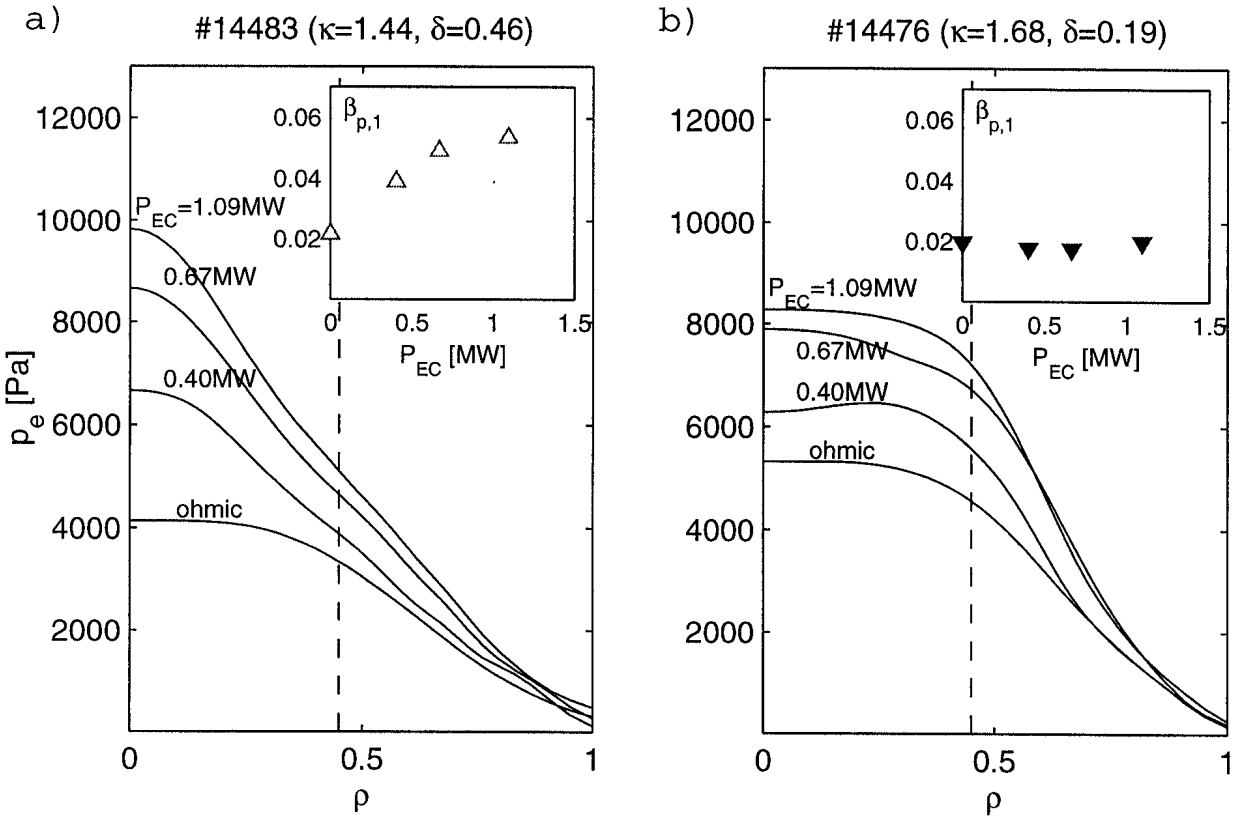

Figure 6: Electron pressure profiles (averaged over typically 6 time slices) for different ECRH powers for a shape ($\kappa = 1.44$, $\delta = 0.46$) where $\tau_{\rm saw}$ increases with heating power (a) and a shape ($\kappa = 1.68$, $\delta = 0.19$) where $\tau_{\rm saw}$ decreases with heating power (b). The inserts show the ECRH power dependence of $\beta_{\rm p}$ at $\rho = 0.45$, corresponding to the inversion radius.

as a function of the triangularity and elongation (Fig. 7(a) and (b)). Despite a large scattering of the data, a stabilizing trend with increasing triangularity and decreasing elongation is observed. The dependence on κ_1 can be compared to an expansion of the energy functional of the ideal internal kink [5]

$$\begin{aligned} \delta\hat{W}_{\rm MHD} = & - \frac{3}{4}(\kappa_1 - 1)\beta_{\rm p,1} \\ & + \Delta q \left[\frac{13}{48} - 3\beta_{\rm p,1}^2 + \frac{\kappa_1 - 1}{2}\left(13\beta_{\rm p,1}^2 - \frac{1}{4}\beta_{\rm p,1} - 1\right)\right]. \end{aligned} \tag{7}$$

The expansion (Eq. (7)) contains terms up to the second order of ϵ and first order of e, including $O(\epsilon^2 e)$ and is given for a parabolic current profile. The value of $\beta_{\rm p,1}$ for marginal stability, calculated from Eq. (7) assuming $\Delta q = 0.1$, is shown in Fig. 7(b). The experimental limiting $\beta_{\rm p,1}$ shows the same trend as the analytic $\beta_{\rm p,1,crit}$, albeit with a weaker dependence.

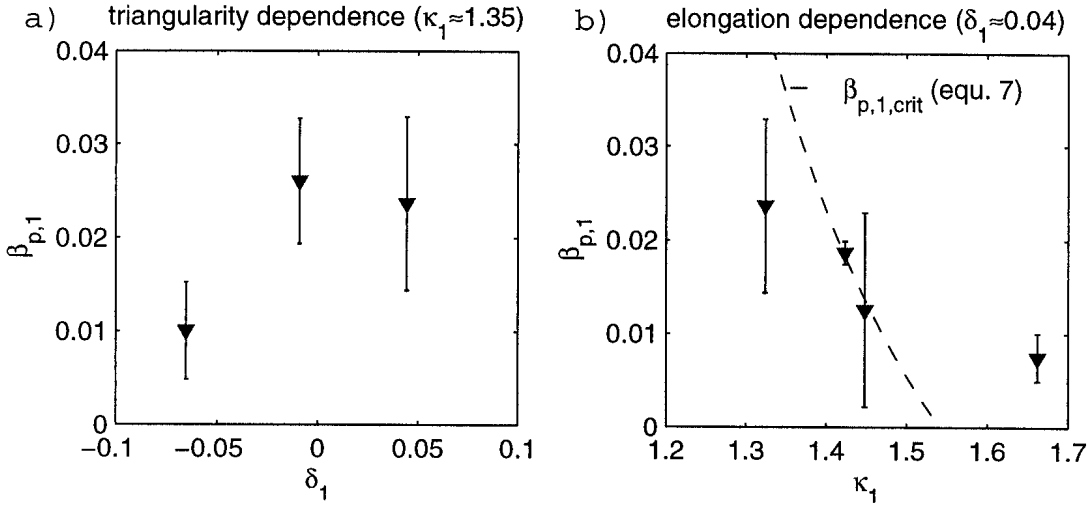

Figure 7: The poloidal beta on q=1 in discharges, where it could not be increased with additional heating, is shown as a function of triangularity (a) and elongation (b) on the q=1 surface. The measurements are averaged over typically 6 times and the error bars indicate the standard deviation among different power levels. It is compared with the poloidal beta for marginal stability of the ideal internal kink according to Eq. (7), assuming $\Delta q = 0.1$ (dashed line in (b)).

5 Summary and conclusion

High triangularities and low elongation are seen to improve the stability of sawteeth in TCV plasmas, but also lead to large sawtooth crashes. High elongation and low triangularity reduce the sawtooth amplitude, which can both reduce sawtooth related heat pulses and decrease the risk of possible seed island generation resulting from large sawtooth crashes. However the core confinement remains at a low level.

Besides their period and amplitude, the response of sawteeth to a variation of heating power strongly depends on the plasma shape. For the plasma shapes for which ideal MHD predicts a low critical $\beta_{p,1}$, the experiment also shows a low pressure limit, which cannot be increased with additional heating and consequently leads to shorter sawteeth. In the frame of the presented model of the sawtooth trigger [6], this is consistent with an ideal internal kink mode triggering the sawtooth crash. In particular the κ_1-dependence of the limiting beta is in qualitative agreement with an analytic prediction [5]. For shapes where the ideal MHD mode is expected to be marginal or stable, in particular at high positive triangularity, the core pressure can be significantly increased with additional heating. This can be explained by an increase of the electron diamagnetic rotation which is expected to increase with the electron pressure and has a stabilizing effect on the resistive mode. However, a prediction of the sawtooth period has to take into account the evolution of the current profile, which has been successfully done for ohmic TCV plasmas [17]. As shown

in the present article, the simulations of sawteeth in ECRH heated TCV plasmas require an accurate description of the shape dependence of ideal MHD stability.

These experiments suggest that in low density TCV plasmas at low triangularity and sufficient elongation ideal MHD significantly contributes to the triggering of the sawtooth crash. In this regime, the observed shape dependence supports theoretical predictions of the shape dependence of the ideal internal kink mode [5].

Acknowledgments

The authors wish to acknowledge the competent support of the whole TCV team. In particular we would like to thank R. Behn and I. Furno for providing experimental data, J.-Ph. Hogge and A. Sushkov for the analysis of the power deposition localization and H. Lütjens and F. Porcelli for helpful discussions. This work was partly funded by the Fonds National Suisse de la Recherche Scientifique.

References

[1] Von Goeler S, Stodiek W and Sauthoff N 1974 *Phys. Rev. Lett.* **33** 1201

[2] Weisen H et al 1997 *Nucl. Fusion* **37** 1741

[3] Pochelon A et al 1999 *Proc. 26th EPS Conf. on Controlled Fusion and Plasma Physics (Maastricht, 1999)* vol 23J ed B Schweer, G Van Oost and E Vietzke (Mulhouse: EPS) p 1089

[4] Bussac M N, Pellat R, Edery D and Soulé J L 1975 *Phys. Rev. Lett.* **35** 1638

[5] Wahlberg C 1998 *Phys. Plasmas* **5** 1387

[6] Porcelli F, Boucher D and Rosenbluth M N 1996 *Plasma Phys. Control. Fusion* **38** 2163

[7] Weisen H, Behn R, Furno I, Moret J-M, Sauter O and TCV team 1998 *Plasma Phys. Control. Fusion* **40** 1803

[8] Furno I, Weisen H, Moret J M, Blanchard P and Anton M 1997 *Proc. 24th EPS Conf. on Controlled Fusion Plasma Physics (Berchtesgaden, 1997)* vol 21A ed M Schittenhelm, R Bartiromo and F Wagner (Geneva: EPS) part II p 545

[9] Hofmann F, Tonetti G 1988 *Nucl. Fusion* **28** 1871

[10] Behn R, Franke S, Pietrzyk Z A, Anton M, Nieswand C, Weisen H and Marlétaz B 1995 *Proc. 7th Int. Symp. Laser Aided Plasma Diagnostics (Fukuoka, Japan 1995)* ed K Muruoka p 392

[11] Goodman T P, Alberti S, Henderson M A, Pochelon A and Tran M Q 1997 *Proc. 19th Symp. on Fusion Technology (Lisbon, 1996)* vol 1 ed C Varandas and F Serra (Amsterdam: Elsevier Science B V) p 565

[12] Pietrzyk Z A et al 1999 *Nucl. Fusion* **39** 587

[13] Pochelon A et al 1999 *Nucl. Fusion (Yokohama Special Issue II)* **39** 1807

[14] Smith G et al 1995 *Proc. 9th joint Workshop on Electron Cyclotron Emission and Electron Cyclotron Heating (Borrego Springs, 1995)*, ed J Lohr (Singapore: World Scientific) p 651

[15] Furno I et al 1999 *Proc. 26th EPS Conf. on Controlled Fusion Plasma Physics (Maastricht, 1999)* vol 23J ed B Schweer, G Van Oost and E Vietzke (Mulhouse: EPS) p 1069

[16] Lütjens H, Bondeson A and Vlad G 1992 *Nucl. Fusion* **32** 1625

[17] Sauter O, Angioni C, Boucher D, Furno I, Pochelon A and Porcelli F 1999 in *Theory of Fusion Plasmas, Proc. of the joint Varenna-Lausanne Int. Workshop (Varenna, 1998)* ed J W Connor, E Sindoni and J Vaclavik (Bologna: Editrice Compositori) p 403